AD-A081 618 ARMY ARMAMENT RESEARCH AND DEVELOPMENT COMMAND ABERD--ETC F/G 19/4
FRACTURE OF ROLLED HOMOGENEOUS STEEL ARMOR (NUCLEATION THRESHOL--ETC(U)
JAN 80 G L MOSS, L SEAMAN

UNCLASSIFIED ARBRL-MR-02984 SBIE-AD-E430 380 NL

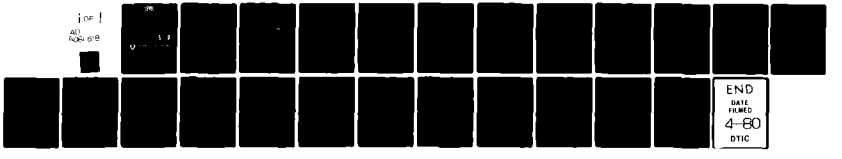

END
DATE FILMED
4-80
DTIC

(12) LEVEL III

AD-E430 380

AD

MEMORANDUM REPORT ARBRL-MR-02984

FRACTURE OF ROLLED HOMOGENEOUS STEEL ARMOR (NUCLEATION THRESHOLD STRESS)

Gerald L. Moss
Lynn Seaman

January 1980

US ARMY ARMAMENT RESEARCH AND DEVELOPMENT COMMAND
BALLISTIC RESEARCH LABORATORY
ABERDEEN PROVING GROUND, MARYLAND

Approved for public release; distribution unlimited.

80 3 05 057

Destroy this report when it is no longer needed.
Do not return it to the originator.

Secondary distribution of this report by originating or sponsoring activity is prohibited.

Additional copies of this report may be obtained from the National Technical Information Service, U.S. Department of Commerce, Springfield, Virginia 22151.

The findings in this report are not to be construed as an official Department of the Army position, unless so designated by other authorized documents.

The use of trade names or manufacturers' names in this report does not constitute indorsement of any commercial product.

UNCLASSIFIED

SECURITY CLASSIFICATION OF THIS PAGE (When Data Entered)

REPORT DOCUMENTATION PAGE	READ INSTRUCTIONS BEFORE COMPLETING FORM
1. REPORT NUMBER (14) Memorandum Report ARBRL-MR-02984	2. GOVT ACCESSION NO. / 3. RECIPIENT'S CATALOG NUMBER
4. TITLE (and Subtitle) (6) Fracture of Rolled Homogeneous Steel Armor (Nucleation Threshold Stress)	5. TYPE OF REPORT & PERIOD COVERED (9) Final rept. / 6. PERFORMING ORG. REPORT NUMBER
7. AUTHOR(s) (10) Gerald L. Moss Lynn Seaman (SRI International)	8. CONTRACT OR GRANT NUMBER(s) (16)
9. PERFORMING ORGANIZATION NAME AND ADDRESS US Army Ballistic Research Laboratory (ATTN: DRDAR-BLT) Aberdeen Proving Ground, MD 21005	10. PROGRAM ELEMENT, PROJECT, TASK AREA & WORK UNIT NUMBERS Proj. Element 6.11.02A DA Proj. No. 1L161102AH43 AMCMS Code 611102.H4300
11. CONTROLLING OFFICE NAME AND ADDRESS US Army Armament Research & Development Command US Army Ballistic Research Laboratory (DRDAR-BL) Aberdeen Proving Ground, MD 21005	12. REPORT DATE (11) JAN [redacted]80 / 13. NUMBER OF PAGES 22
14. MONITORING AGENCY NAME & ADDRESS (if different from Controlling Office) (12) 24	15. SECURITY CLASS. (of this report) Unclassified / 15a. DECLASSIFICATION/DOWNGRADING SCHEDULE N/A

16. DISTRIBUTION STATEMENT (of this Report)

Approved for public release; distribution unlimited.

(18) SBIE (19) AD-E430 380

17. DISTRIBUTION STATEMENT (of the abstract entered in Block 20, if different from Report)

18. SUPPLEMENTARY NOTES

19. KEY WORDS (Continue on reverse side if necessary and identify by block number)

Crack, Crack nucleation stress, Crack threshold stress, Fracture, Fracture stress, Spallation, Armor, Rolled homogeneous steel armor

20. ABSTRACT (Continue on reverse side if necessary and identify by block number) bet Ext. 2972

Methods of characterizing the onset of fracture of rolled homogeneous steel armor with stress waves were investigated, and the nucleation threshold stress was determined to be 1.65 GPa.

Crack nucleation was associated with the emergence and propagation of "hair-line" cracks from inclusion-matrix interfaces, and the nucleation threshold stress applies to this condition.

(OVER)

DD FORM 1 JAN 73 1473 EDITION OF 1 NOV 65 IS OBSOLETE

UNCLASSIFIED 393471

SECURITY CLASSIFICATION OF THIS PAGE (When Data Entered)

To determine this value accurately, the tensile stresses in regions of failure were obtained with the aid of the BFRACT 2 computer subroutine containing the nucleation and growth fracture model, NAG/FRAG. This automatically accounts for the unloading of stress as voids develop and allows one to determine approximately the tensile stress responsible for failure. Crack densities created with plate impacts were plotted versus the corresponding computed maximum tensile stresses, and the curve was extrapolated to the no-damage condition, i.e., the stress below which no cracks should develop. This stress level was equated to the nucleation threshold stress.

The nucleation threshold stress that has been determined is a material parameter in the NAG/FRAG analysis of dynamic fracture, and it should, therefore, be useful in the prediction of damage and fragmentation for vulnerability analyses of Army hardware.

TABLE OF CONTENTS

I. INTRODUCTION

There has been a long-standing requirement for a detailed description of the mass, velocity and size distributions of fragments created during projectile impact on armor targets. This information is required for an interpretation of the damage a fragment cloud could cause a secondary target.

Previously, information about fragment debris has only been obtainable through expensive experimentation, but within the last two decades, there has been substantial progress in the development of an active fracture model (NAG/FRAG)[1-3] that is essentially sufficient for the prediction of exactly the fragment information desired.

The complete fracture model is based on the nucleation and growth of voids and subsequent void coalescence, i.e., features of failure that are known to occur with the continued application of intense loads. In keeping with experimental observations,[4] fragmentation is treated as the coalescence of voids and is, therefore, dependent on nucleation.

Through investigations of several materials including iron,[2] copper,[5] beryllium[6] and a polycarbonate, Lexan,[7] it has been discovered that the nucleation rate $\dot{N}$ of voids in many materials is exponentially dependent on the applied stress σ and satisfies the relation

---

[1] *G. Moss and C. M. Glass, "Some Microscopic Observations of Cracks Developed in Metals by Very Intense Stress Waves," Ballistic Research Laboratories Technical Note No. 1312, April 1960.* (AD #237943)

[2] *T. Barbee, L. Seaman, and R. C. Crewdson, "Dynamic Fracture Criteria of Homogeneous Materials," Air Force Weapons Laboratory Technical Report No. AFWL-TR-70-99, November 1970.*

[3] *L. Seaman, D. R. Curran, and D. A. Shockey, "Computational Models for Ductile and Brittle Fracture," J. Appl. Phys., Vol. 47, No. 11, November 1976, pp. 4814-4826.*

[4] *D. A. Shockey, L. Seaman, D. R. Curran, P. S. DeCarli, M. Austin, and J. P. Wilhelm, "A Computational Model for Fragmentation of Armor Under Ballistic Impact," Ballistic Research Laboratories Contract Report No. 222, April 1975.* (AD #B004672L)

[5] *L. Seaman, T. W. Barbee, Jr., and D. R. Curran, "Dynamic Fracture Criteria of Homogeneous Materials," Air Force Weapons Laboratory Technical Report No. AFWL-TR-71-156, December 1971.*

[6] *D. A Shockey, L. Seaman, and D. R. Curran, "Dynamic Fracture of Beryllium Under Plate Impact and Correlation with Electron Beam and Underground Test Results," Air Force Weapons Laboratory Technical Report No. AFWL-TR-73-12, June 1973.*

[7] *D. R. Curran, D. A. Shockey, and L. Seaman, "Dynamic Fracture Criteria for a Polycarbonate," J. Appl. Phys. Vol. 44, No. 9, September 1973, p. 4025.*

$$\dot{N} = \dot{N}_o \, e^{(\sigma-\sigma_{no})/\sigma_1} , \qquad (1)$$

where σ_{no} is the threshold stress for the nucleation of voids, and $\dot{N}_o$ and σ_1 are experimentally determined material parameters.

In addition, the fracture model includes equations for the growth and coalescence of voids, and these equations, in turn, depend on independent sets of material parameters.

All the material parameters, including σ_{no}, are usually established simultaneously with a trial-and-error procedure - one in which a set of parameters is assumed and used in a computation to predict the total cracking from specific stress histories. Then, the cracking of samples actually subjected to these loading conditions is determined experimentally and compared with the computed results. The procedure is repeated until there is agreement, which implies the correct parameters have been found, or until continued disagreement suggests the fracture model is being used with inappropriate nucleation and growth functions. When the approach is properly applied, sufficient test data is used to ensure unique results for the range of conditions investigated.

While all the parameters can be found by this trial-and-error procedure, their determination is substantially simplified if σ_{no} is found by an independent method. Such an independent evaluation was attempted and is the subject of this report.

II. PROCEDURE

The material used for these tests was MIL SPEC 12560-B rolled homogeneous steel armor (12.7 mm thick plate) with the composition given in Table I. Mechanical properties of this same plate of steel have been characterized in parallel research efforts to furnish consistent data for this material.[8-10]

---

[8] *R. F. Benck, "Quasi-Static Tensile Stress Strain Curves--II, Rolled Homogeneous Armor," Ballistic Research Laboratories Memorandum Report 2703, November 1976.* (AD #B016015L)

[9] *R. F. Benck and J. L. Robitaille, "Tensile Stress-Strain Curves--III, Rolled Homogeneous Armor at a Strain Rate of 0.42 s^{-1}," Ballistic Research Laboratory Memorandum Report 2760, June 1977.* (AD #A041560)

[10] *G. E. Hauver, "The Alpha-Phase Hugoniot of Rolled Homogeneous Armor," Ballistic Research Laboratories Memorandum Report 2651, August 1976.* (AD #B012871L)

TABLE I

COMPOSITION OF STEEL, WEIGHT PERCENT

C	Mn	P	S	Si	Ni	Cr
0.22	0.26	0.001	0.015	0.19	3.15	1.06
Cu	**V**	**Mo**	**Al**	**B**	**Ti**	
0.1	0.01	0.15/0.30	0.03	N.D.	N.D.	

The microstructure of the material was bainitic with inclusions as shown in Fig. 1. The Rockwell "C" hardness was 37, and the material will, therefore, be referred to in the following as RHA (RC-37).

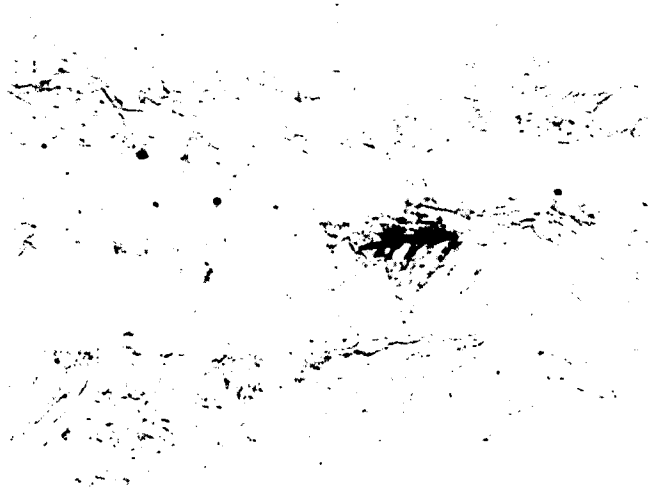

Figure 1. Rolled homogeneous steel armor. Nital etch; magnification 500.

It was considered possible that σ_{no} could be determined independently of the NAG/FRAG model if the density of voids created at several stresses above the nucleation threshold stress were plotted versus the impact compressive stress, and the curve was extrapolated to the stress where no voids would form, i.e., to the no-damage condition.

For such a procedure to work, the need to account for special details normally taken into account by the NAG/FRAG analysis must be overcome. Specifically, the reduction in stress amplitude by elastic wave reflections from a plastic wave front, as occurs when plate impacts are used to cause fracture, and the changes in stress associated with unloading at void interfaces must either be treated independently or be reduced to negligible effects.

The approach used was to try to render the elastic wave reflections from the plastic wave and the unloading at void interfaces negligible by working within a stress range just above the nucleation threshold stress.

There should be only a weak wave reflected from an encounter of elastic and plastic waves when the amplitude of the plastic wave is only slightly greater than the Hugoniot elastic limit.[11] Furthermore, the average effect of unloading at void interfaces should be trivial since only a few small voids would be generated at low stresses. Certainly, the "reflection" effect should go to zero at the elastic-plastic transition stress (EPTS), and the "void interface" effects should go to zero at the nucleation threshold stress.

It has been observed in previous fracture tests that the nucleation threshold stress is often approximately the same as the EPTS, and without exceeding it, there would be little chance of breaking a sample. Hence, the EPTS was taken as the lower bound on the range of shock stresses of interest, and the upper bound was just one GPa higher.

Examples of fracture from impact loading in this stress range were created with parallel plate impacts accomplished with a light-gas gun. The maximum compressive stress from such an impact is given by[10,12]

$$\sigma = \sigma_e + \sigma_p \ , \qquad (2)$$

where σ_e is the amplitude of the elastic precursor that leads the plastic part of the stress wave, and σ_p is the difference between the maximum

---

[11] *T. W. Wright, "Ultrasonic Probing of Plastic Waves," J. Appl. Phys., Vol. 39, No. 12, November 1968, pp. 5740-5745.*

[12] *M. H. Rice, R. G. McQueen, and J. M. Walsh, "Compression of Solids by Strong Shock Waves," Solid State Physics, Vol. 6, F. Seitz and D. Turnbull, Eds., Academic Press, New York, 1958, pp. 1-63.*

amplitude of the plastic wave and σ_e. The stress of the elastic precursor is given by

$$\sigma_e = \rho_o U_e u_e , \tag{3}$$

where U and u designate the stress wave and particle velocities respectively, ρ_o is the initial density of the material and the subscript e refers to the elastic condition. The plastic increment σ_p is given by

$$\sigma_p = \rho_e U_p(u_p - u_e) . \tag{4}$$

Here, the subscript p refers to the plastic condition.

It is well known that u_p is approximately one-half the free surface velocity u_i of a plate striking a stationary plate,[12] and U_e for RHA (RC-37) has been established as 5.83 mm/μsec.[10]

Since σ depends on u_i, impacts at different velocities were used to obtain the desired range of shock stresses.

The samples and targets were 12.7 and 6.4 mm thick, respectively, and with this geometry the maximum tensile stress duration was approximately 1.19 μsec. Fig. 2 shows the approximate maximum stress duration as a function of location in the sample for an impact velocity of 0.118 mm/μsec. This is representative of each of the tests since the plastic wave velocities differed from test to test by at most 0.22 percent.

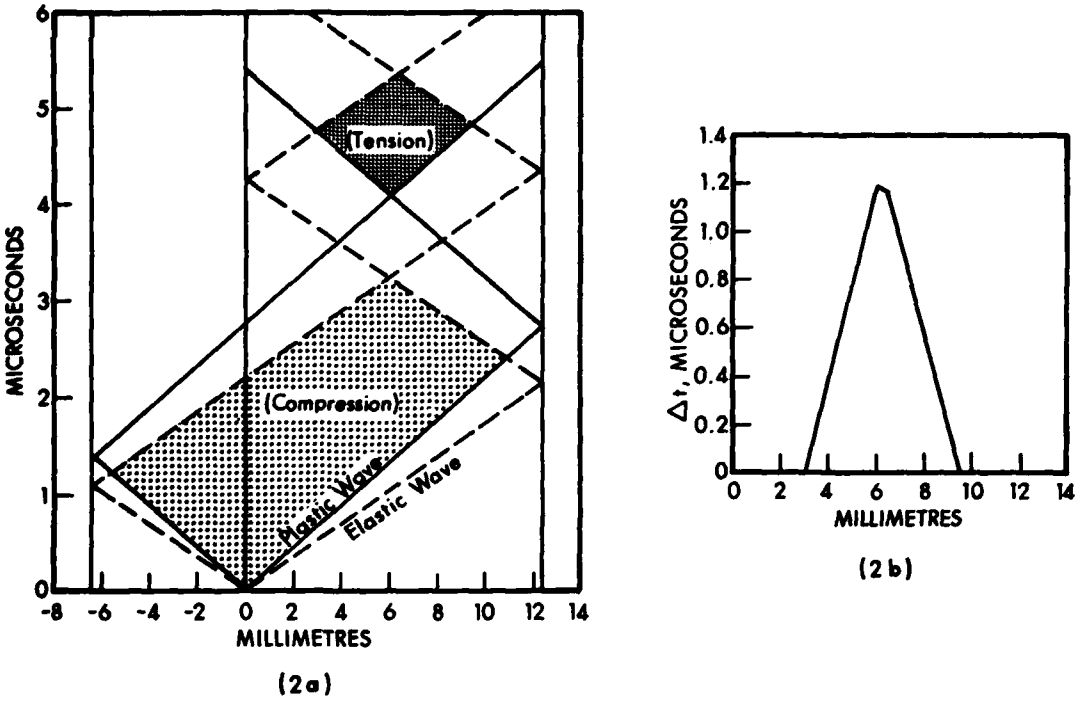

Figure 2. (a) Lagrangian plot of the location of the elastic and plastic wave fronts versus time. (b) Maximum tensile stress duration versus distance through the thickness of the plate-shaped sample.

It has been found experimentally that the elastic-plastic transition stress (EPTS) of shock waves emanating from planar impact interfaces decreases in amplitude with travel.[13] In the case of the 12.7 mm thick samples used, the shock wave traveled 19.1 mm to the zone of maximum tensile stress duration which was roughly where maximum damage should be expected. After a shock wave travels 19.1 mm in RHA (RC-37), the EPTS drops to about 1.9 GPa.[10] Hence, this was selected as the lower bound on the impact pressures of interest.

A summary of the impact velocities and the resultant maximum compressive stress levels is given in Table II.

[13] *B. M. Butcher and D. E. Munson, "The Application of Dislocation Dynamics to Impact-Induced Deformation Under Uniaxial Strain," Dislocation Dynamics, A. R. Rosenfield, G. T. Hahn, A. L. Bement, Jr. and R. I. Jaffee, Eds., McGraw-Hill Book Co., New York, 1968, pp. 591-607.*

TABLE II TEST CONDITIONS USED TO ESTABLISH σ_{no}	
IMPACT VELOCITY mm/μsec.	MAXIMUM COMPRESSIVE STRESS GPa
0.0954	2.08
0.1178	2.49
0.1392	2.88

In this work, the impact velocities were measured, and the stresses listed in Table II were determined with Eqs. 2 through 4 and the Hugoniot relation[10]

$$U_p = 4.51 + 1.43\, u_p \qquad (5)$$

III. RESULTS

Observation of the recovered and sectioned samples revealed they were all partially broken by the impacts and that the nature of the failure was the same in all the samples. However, the voids in the low-pressure test were confined entirely to a narrow region at the midplane of the plate.

Microscopic observation of the sectioned samples revealed the breaking process was one in which (1) inclusions cracked or became separated from the matrix, (2) "hair-line" cracks extended into the matrix from the damaged inclusions - while under load, these cracks were presumably open, (3) the "hair-line" cracks extended from inclusion to inclusion and (4) cracks on slightly separated planes coalesced by shear deformation on surfaces connecting the ends of the cracks.

Clearly, there are several distinct stages in the failing process, and nucleation can be interpreted in several ways. For example, a stable nucleus could quite naturally be envisioned as a cracked inclusion. Here, however, nucleation was associated with the development of the "hair-line" cracks that extended from inclusions into the matrix. Hence, cracks were not intentionally counted until they had reached this stage of development.

Identifying and counting cracks in this way is a useful way to keep track of the damage to RHA because the "hair-line" cracks must nucleate and grow before the material can separate into pieces.

Actually, the connection of voids by plastic shear is the last feature of the breaking process, but the heating on these shear zones by plastic working results in weakened material on which further separation can occur relatively easily. It is convenient, therefore, to identify this stage of failure with coalescence and to treat it with a recently developed fragmentation analysis.[4] Hence, voids connected by shear were counted as two cracks when separated by approximately one-third the distance between the faces of the most open crack.

Eq. (1), if applicable, implies that nucleation continues as long as a stress greater than σ_{no} is applied. Furthermore, it is clear from Fig. 2 that the load duration depended on the location in the plate. Hence, only voids from the central regions of each plate were counted. For the 1.93 GPa test, this was a region 0.066 cm (0.026 in.) wide centered about the maximum damage in the plate. For the other tests, this was a region 0.127 cm (0.05 in.) wide, also centered about the maximum damage. This ensured the voids from each test were initiated over equal time intervals and allowed the use of data from the low pressure test - an advantage in reducing the extent of an extrapolation to the nucleation threshold stress.

A graph of the total number of voids counted in these central regions versus the maximum compressive stresses imposed on the samples is shown in Fig. 3.

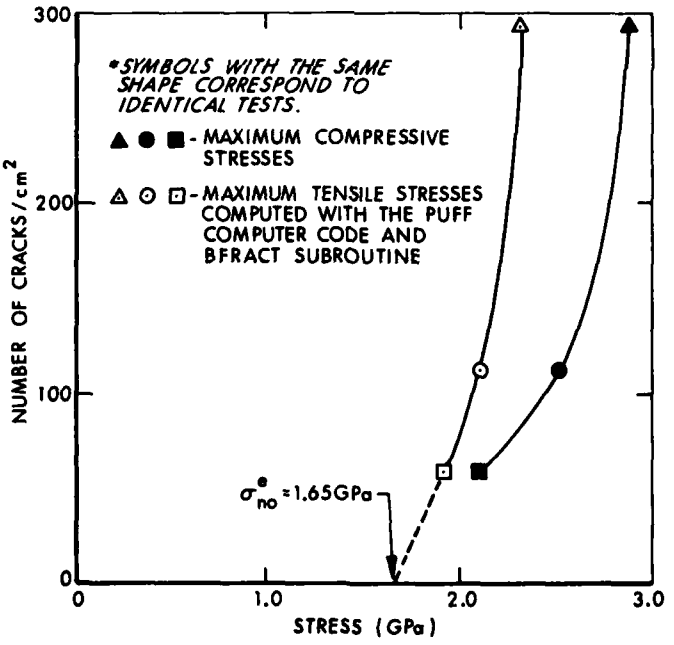

Figure 3. Stress dependence of void densities in the regions of maximum damage - approximately the midplane of each sample.

IV. DISCUSSION

It was not known before examining the results if the stress range selected for this work was sufficiently near the nucleation threshold stress to make the impact compressive stresses a good approximation of the maximum tensile stresses developed. This was, therefore, checked by computing the maximum tensile stresses with the one-dimensional wave-propagation computer program PUFF and the brittle fracture subroutine BFRACT 2.[4,14] Such a computation automatically accounts for the elastic-plastic wave interactions as well as the development of voids.

The occurrence and development of voids is treated simultaneously with the loading history which is the only way predictions of the process can be made because failure and loading are interdependent processes. The failure (development of cracks) that occurs and the corresponding adjustment in the load (stresses) are based on the volume change ΔV imposed on the sample. It is assumed that this change is a composite of the volume change by strain in the solid ΔV_s, volume change due to nucleation ΔV_n and volume change by void growth and expansion ΔV_g. When expressed in these terms, the volume change is given by[4]

$$\Delta V = \Delta V_s + \Delta V_n + \Delta V_g \quad . \tag{6}$$

The change in solid volume ΔV_s during the computation time increment is related to the pressure in the solid P_s which is obtained from the Mie-Grüneisen relation[4]

$$P_s = C \frac{1}{\rho_o\left(V_{so} + \Delta V_s\right)} + \frac{\Gamma E}{V_{so} + \Delta V_s} \quad , \tag{7}$$

where C is the bulk modulus, Γ is the Grüneisen ratio, E is the internal energy and the subscript "o" refers to conditions at the beginning of the time increment.

The increment of nucleated void volume ΔV_n is determined from the product of the number of voids nucleated during the time increment (Eq. 1) and the volume of the voids. The growth increment ΔV_g is based on both the increase in crack radius and the elastic opening of the crack. Together, the three terms ΔV_s, ΔV_n and ΔV_g are related in complex ways to the applied stress so that the stress cannot be obtained directly for the imposed strain increments.

---

[14] *L. Seaman, "SRI PUFF 8 Computer Program for One-Dimensional Stress Wave Propagation," Ballistic Research Laboratory Contract Report (Being Printed).*

The solution for stress is obtained by an iteration procedure in which a stress tensor is first estimated. Then, the three increments on the right side of Eq. 6 are obtained directly. The sum of these increments is ΔV_a, an approximation of ΔV. Repeated stress estimates are made with a regula falsi method until ΔV_a is sufficiently close to ΔV. Results are made reasonably independent of step size by requiring that[4]

$$\left(\Delta V - \Delta V_a\right)/V_s < 2 \times 10^{-5} , \qquad (8)$$

where ΔV_a is one of the iterative estimates of the volume change. It has been found that when this inequality is satisfied, results are independent of step size to a precision of 0.003 GPa.

When applying the BFRACT model, it is important to represent the crack nucleation rate correctly. This was assumed to be given by Eq. 1 which is consistent with the material behavior if, for constant load durations, ln N versus σ is a straight line. The crack densities shown in Fig. 3 were obtained from regions of maximum damage for which the load duration was essentially the same in each test, and when the data is replotted as in Fig. 4, it is clear that the material behavior is represented very well by Eq. 1. Hence, the method of calculating the tensile stresses was reasonable.

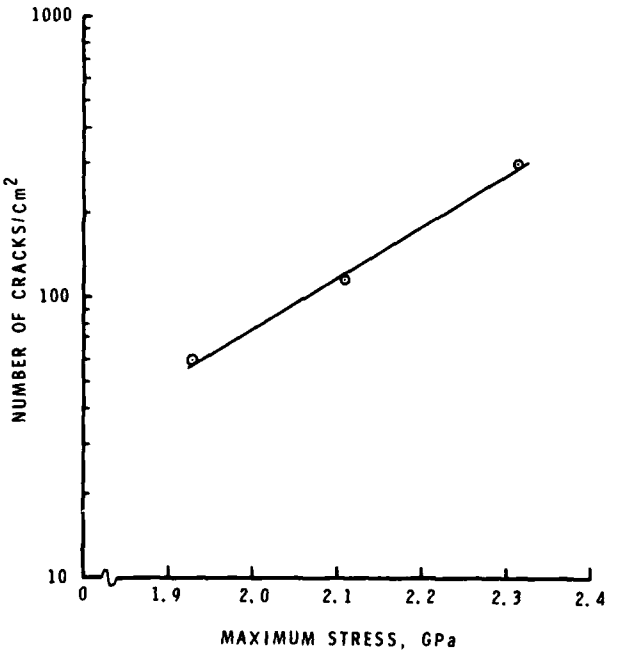

Figure 4. Damage caused by tensile stress waves at the midplane of samples.

The computed tensile stresses are shown in Fig. 3, and it is evident that they are less than the impact pressures. Furthermore, the difference in these stresses increases with the intensity of the load. Hence, an extrapolation of the compressive stresses to the no-damage condition would give a substantially incorrect value for σ_{no}.

Presumably, the compressive stresses could still be used in an extrapolation to the no-damage condition provided useful data were obtained from tests conducted at stresses below 2 GPa. However, experimental evidence suggests this would be impractical for RHA (RC-37) because the cracks formed are so widely spaced when maximum stresses are in this range that it would be difficult to determine meaningful average crack densities.

Hence, it is concluded that it is not possible to use an extrapolation independent of an "active" fracture analysis to determine σ_{no} for RHA (RC-37).

It is, however, useful to extrapolate the crack density against tensile stress to the no-damage condition because the nucleation threshold stress established with this procedure necessarily corresponds to the stress where failure begins. In contrast, the "trial-and-error" procedure used to determine the nucleation and growth material parameters is based on the best fit of observable fracture data, but these are developed with loading conditions that do not include the stress where fracture begins.

The suggested extrapolation is shown in Fig. 3, and the nucleation threshold stress σ_{no}^{e} corresponding to the no-damage condition is 1.65 GPa.

The result of a trial-and-error determination, σ_{no}^{te}, was 1.8 GPa. The two results are different because in determing σ_{no}^{te} the density of cracks with radii less than 0.15 mm were underestimated because the size distribution curve ($\ln N_c$ vs. R) was nonlinear in the size range $0 < R < 0.60$ mm and more complicated than could be described with the model at hand. Cracks with radii between 0.15 and 0.60 mm were, however, represented correctly.

The result of the extrapolation should only be in error to the extent that cracks with radii in the range $0 < R < 0.15$ mm were ignored while computing the tensile stresses with the PUFF-BFRACT computer code. This error should be small because these voids contribute little to the total void volume. Hence, the actual nucleation threshold stress of 1.65 GPa should be reasonably accurate.

As already indicated, the EPTS at the midplane of the samples was 1.9 GPa. Thus, it appears that cracks nucleated at stresses below the yield stress of the material. This could be due to moderate stress

concentrations at inclusions or the method that has been used to determine the EPTS.[10]

The EPTS, as reported in Reference 10, was determined by extending the straight line portions of the stress wave profile (free surface velocity vs. time) on adjacent sides of the transition. The intersection of these straight lines was reported as the EPTS. However, in the case of RHA (RC-37) there is actually a gradual change in the stress wave at the EPTS, and the first deviation in linearity in the elastic precursor could be an indication of the first yielding to occur. For example, the reported EPTS after a stress wave has traveled 9.51 mm in RHA (RC-37) is 2.09 GPa,[10] while the stress corresponding to the first deviation from an approximately linear increase in stress at the elastic wave front is 1.77 GPa. A proportional adjustment in the EPTS, which was 1.9 GPa at the region of maximum fracture, suggests yielding started at 1.61 GPa which is less than the nucleation threshold stress of 1.65 GPa - a reasonable result.

V. CONCLUSION

A nucleation threshold stress σ_{no} of 1.65 GPa was established for the creation of cracks in rolled homogeneous steel armor (RC-37) with impulsive loading.

The failure of this material progresses by inclusion cracking, followed in succession by the growth of "hair-line" cracks away from regions of broken inclusions, in-plane crack extension from inclusion to inclusion and coalescence of non-planar cracks by shear on connecting surfaces.

The nucleation threshold stress of 1.65 GPa corresponds to the initiation of the "hair-line" cracks.

The approach used to establish σ_{no} depended on extrapolating crack densities developed over a range of pressures to the no-damage condition. It was found that this procedure makes sense, but the tensile stresses that cause failure must be used rather than the impact compressive stresses. It was found that the tensile stresses are substantially less than the compressive stresses because of elastic wave reflections and unloading at void interfaces. These factors were accounted for in this work with computations based on the PUFF computer code and the BFRACT subroutine.

REFERENCES

1. G. Moss and C. M. Glass, "Some Microscopic Observations of Cracks Developed in Metals by Very Intense Stress Waves," Ballistic Research Laboratories Technical Note No. 1312, April 1960. (AD #237943)

2. T. Barbee, L. Seaman, and R. C. Crewdson, "Dynamic Fracture Criteria of Homogeneous Materials," Air Force Weapons Laboratory Technical Report No. AFWL-TR-70-99, November 1970.

3. L. Seaman, D. R. Curran, and D. A. Shockey, "Computational Models for Ductile and Brittle Fracture," J. Appl. Phys., Vol. 47, No. 11, November 1976, pp. 4814-4826.

4. D. A. Shockey, L. Seaman, D. R. Curran, P. S. DeCarli, M. Austin, and J. P. Wilhelm, "A Computational Model for Fragmentation of Armor Under Ballistic Impact," Ballistic Research Laboratories Contract Report No. 222, April 1975. (AD #B004672L)

5. L. Seaman, T. W. Barbee, Jr., and D. R. Curran, "Dynamic Fracture Criteria of Homogeneous Materials," Air Force Weapons Laboratory Technical Report No. AFWL-TR-71-156, December 1971.

6. D. A. Shockey, L. Seaman, and D. R. Curran, "Dynamic Fracture of Beryllium Under Plate Impact and Correlation with Electron Beam and Underground Test Results," Air Force Weapons Laboratory Technical Report No. AFWL-TR-73-12, June 1973.

7. D. R. Curran, D. A. Shockey, and L. Seaman, "Dynamic Fracture Criteria for a Polycarbonate," J. Appl. Phys., Vol. 44, No. 9, September 1973, p. 4025.

8. R. F. Benck, "Quasi-Static Tensile Stress Strain Curves--II, Rolled Homogeneous Armor," Ballistic Research Laboratories Memorandum Report 2703, November 1976. (AD #B016015L)

9. R. F. Benck and J. L. Robitaille, "Tensile Stress-Strain Curves--III, Rolled Homogeneous Armor at a Strain Rate of 0.42 s^{-1}," Ballistic Research Laboratory Memorandum Report 2760, June 1977. (AD #A041560)

10. G. E. Hauver, "The Alpha-Phase Hugoniot of Rolled Homogeneous Armor," Ballistic Research Laboratories Memorandum Report 2651, August 1976. (AD #B012871L)

11. T. W. Wright, "Ultrasonic Probing of Plastic Waves," J. Appl. Phys., Vol. 39, No. 12, November 1968, pp. 5740-5745.

12. M. H. Rice, R. G. McQueen, and J. M. Walsh, "Compression of Solids by Strong Shock Waves," Solid State Physics, Vol. 6, F. Seitz and D. Turnbull, Eds., Academic Press, New York, 1958, pp. 1-63.

13. B. M. Butcher and D. E. Munson, "The Application of Dislocation Dynamics to Impact-Induced Deformation Under Uniaxial Strain," Dislocation Dynamics, A. R. Rosenfield, G. T. Hahn, A. L. Bement, Jr. and R. I. Jaffee, Eds., McGraw-Hill Book Co., New York, 1968, pp. 591-607.

14. L. Seaman, "SRI PUFF 8 Computer Program for One-Dimensional Stress Wave Propagation," Ballistic Research Laboratory Contract Report (Being Printed).

DISTRIBUTION LIST

No. of Copies	Organization
12	Commander Defense Technical Info Center ATTN: DDC-DDA Cameron Station Alexandria, VA 22314
4	Director Defense Advanced Research Projects Agency ATTN: Tech Info Dr. Ernest F. Blase Dr. Bement Dr. Ray Gogolewski 1400 Wilson Boulevard Arlington, VA 22209
1	Deputy Assistant Secretary of the Army (R&D) Department of the Army Washington, DC 20310
1	Commander US Army War College ATTN: Lib Carlisle Barracks, PA 17013
1	Commander US Army Command and General Staff College ATTN: Archives Fort Leavenworth, KS 66027
1	Commander US Military Academy ATTN: Library West Point, NY 10996
1	Commander US Army Materiel Development and Readiness Command ATTN: DRCDMD-ST 5001 Eisenhower Avenue Alexandria, VA 22333
6	Commander US Army Armament Research and Development Command ATTN: DRDAR-TSS (2 cys) J.D. Corrie R.J. Weimer J. Beetle E. Bloore Dover, NJ 07801
1	Commander US Army Armament Materiel Readiness Command ATTN: DRSAR-LEP-L, Tech Lib Rock Island, IL 61299
1	Director US Army ARRADCOM Benet Weapons Laboratory ATTN: DRDAR-LCB-TL Watervliet, NY 12189
5	Commander US Army Watervliet Arsenal ATTN: Dr. T. Davidson Dr. M.A. Hussain Dr. S.L. Pu Dr. John Underwood Mr. D.P. Kendall Watervliet, NY 12189
1	Commander US Army Aviation Research and Development Command ATTN: DRSAV-E P.O. Box 209 St. Louis, MO 63166
1	Director US Army Air Mobility Research and Development Laboratory Ames Research Center Moffett Field, CA 94035

DISTRIBUTION LIST

No. of Copies	Organization
1	Commander US Army Communications Research and Development Command ATTN: DRDCO-PPA-SA Fort Monmouth, NJ 07703
1	Commander US Army Electronics Research and Development Command Technical Support Activity ATTN: DELSD-L Fort Monmouth, NJ 07703
1	Commander US Army Harry Diamond Labs ATTN: DRXDO-TI 2800 Powder Mill Road Adelphi, MD 20783
3	Commander US Army Missile Command ATTN: DRDMI-R DRDMI-YDL Dr. Raymond Conrad Redstone Arsenal, AL 35809
3	Commander US Army Mobility Equipment Research & Development Cmd ATTN: DRDME-WC DRSME-RZT STSFB-MW, Dr.J. Bond Fort Belvoir, VA 22060
1	Commander US Army Tank Automotive Research and Development Command ATTN: DRDTA-UL Warren, MI 48090
4	Commander US Army Materials and Mechanics Research Center ATTN: DRXMR-ATL DRXMR-H, Dr. D. Dandekar DRXMR-T, Mr. J. Mescall DRXMR-H, Dr. S.C. Chou Watertown, MA 02172
4	Commander US Army Research Office ATTN: Dr. Hermann Robl Dr. E. Saibel Dr. George Mayer Dr. James Murray P.O. Box 12211 Research Triangle Park NC 27709
1	Commander US Army Research and Standardization Group (Europe) ATTN: Dr. B. Steverding Box 65 FPO NY 09510
1	Director US Army TRADOC Systems Analysis Activity ATTN: ATAA-SL, Tech Lib White Sands Missile Range NM 88002
1	Office of Naval Research ATTN: Code 402 Department of the Navy Washington, DC 20360
2	Commander Naval Surface Weapons Ctr ATTN: Mr. W.H. Holt Tech Lib Dahlgren, VA 22445

DISTRIBUTION LIST

No. of Copies	Organization
2	Commander Naval Surface Weapons Ctr ATTN: Dr. Robert Crowe Tech Lib Silver Spring, MD 20910
1	Commander Naval Research Laboratory ATTN: Code 2020, Tech Lib Washington, DC 20375
7	Commander Naval Research Laboratory Engineering Materials Division ATTN: E.A. Lange G.R. Yoder C.A. Griffis R.J. Goode R.W. Judy, Jr. A.M. Sullivan T.W. Crooker Washington, DC 20375
1	Commander Naval Research Laboratory Metallurgy Division ATTN: W.S. Pellini Washington, DC 20375
1	AFOSR (Dr. Alan H.Rosenstein) Bolling AFB, DC 20332
1	AFWL (Tech Lib) Kirtland AFB, NM 87117
1	Director Lawrence Livermore Laboratory ATTN: Dr. M.L. Wilkins P.O. Box 808 Livermore, CA 94550
6	Sandia Laboratories ATTN: Tech Lib Dr. A.L. Stevens Dr. Lee Davison Dr. W.E. Warren Dr. L.D. Bertholf Dr. Marlin Kipp Albuquerque, NM 87115
4	SRI International ATTN: Dr. George R. Abrahamson Dr. Donald R. Curran Dr. Donald A. Shockey Dr. Lynn Seaman 333 Ravenswood Avenue Menlo Park, CA 94025
1	Terra Tek, Inc. ATTN: Dr. Arfon Jones 420 Wahara Way University Research Park Salt Lake City, UT 84108
1	Brown University Division of Applied Mathematics ATTN: Prof. H. Kolsky Providence, RI 02912
2	Brown University Division of Engineering ATTN: Prof. James R. Rice Prof. L.B. Freund Providence, RI 02912
1	Colorado School of Mines Dept of Metallurgical Engr. ATTN: Prof. George Krauss Golden, CO 80401
1	Drexel University Dept of Materials Engineering ATTN: Prof. Harry C. Rogers Philadelphia, PA 19104

DISTRIBUTION LIST

No. of Copies	Organization
2	The Johns Hopkins University ATTN: Prof. R.B. Pond, Sr. Prof. R. Green 34th and Charles Streets Baltimore, MD 21218
1	Lehigh University Institute of Fracture and Solid Mechanics ATTN: Prof. George C. Sih Bethlehem, PA 18015
1	Lehigh University Department of Mechanics ATTN: Prof. Frazil Erdogen Bethlehem, PA 18015
1	Massachusetts Inst of Tech ATTN: Prof. Frank A. McClintock 77 Massachusetts Avenue Cambridge, MA 02139
2	Michigan Technological Univ. Dept of Metallurgical Engr. ATTN: Prof. Dale F. Stein Prof. Donald E. Mikkola Houghton, MI 49931
1	South Dakota State University Dept of Mechanical Engineering ATTN: Prof. Michael P. Wnuk Brookings, SD 57006
1	Union College ATTN: Prof. Raymond Eisenstadt Schenectady, NY 12308
2	University of California Los Alamos Scientific Lab ATTN: Dr. W.E. Deal, Jr. Tech Lib P.O. Box 1663 Los Alamos, CA 87545
1	University of Illinois Department of Teoretical and Applied Mechanics College of Engineering ATTN: Prof. Herbert T. Corten Urbana, IL 61801
1	University of Notre Dame Dept of Metallurgical Engineering and Materials Sciences ATTN: Prof. N.F. Fiore Notre Dame, IN 46556
1	University of Pittsburgh ATTN: Dean M.L. Williams Pittsburgh, PA 15213
1	University of Washington Department of Mechanical Engineering ATTN: Prof. A.S. Kobayashi Seattle, WA 98105
1	Washington State University Department of Physics ATTN: Prof. G.E. Duvall Pullman, WA 99163
	Aberdeen Proving Ground
	Dir, USAMSAA ATTN: DRXSY-D DRXSY-MP, H. Cohen Cdr, USATECOM ATTN: DRSTE-TO-F Bldg 314
	Dir, Wpns Sys Concepts Team, Bldg. E3516, EA ATTN: DRDAR-ACW

USER EVALUATION OF REPORT

Please take a few minutes to answer the questions below; tear out this sheet and return it to Director, US Army Ballistic Research Laboratory, ARRADCOM, ATTN: DRDAR-TSB, Aberdeen Proving Ground, Maryland 21005. Your comments will provide us with information for improving future reports.

1. BRL Report Number _____

2. Does this report satisfy a need? (Comment on purpose, related project, or other area of interest for which report will be used.)

_____

_____

_____

3. How, specifically, is the report being used? (Information source, design data or procedure, management procedure, source of ideas, etc.) _____

_____

_____

4. Has the information in this report led to any quantitative savings as far as man-hours/contract dollars saved, operating costs avoided, efficiencies achieved, etc.? If so, please elaborate.

_____

_____

5. General Comments (Indicate what you think should be changed to make this report and future reports of this type more responsive to your needs, more usable, improve readability, etc.) _____

_____

_____

_____

6. If you would like to be contacted by the personnel who prepared this report to raise specific questions or discuss the topic, please fill in the following information.

Name: _____

Telephone Number: _____

Organization Address: _____

_____

_____